

## Article

# Design and Synthesis of New Anthranil Phenylhydrazides: Antileishmanial Activity and Structure–Activity Relationship

Claudia do Carmo Maquiaveli <sup>1,\*</sup>, Edson Roberto da Silva <sup>1,\*</sup> , Barbara Hild de Jesus <sup>1</sup>,  
Caio Eduardo Oliveira Monteiro <sup>1</sup>, Tiago Rodrigues Navarro <sup>2</sup>, Luiz Octavio Pereira Branco <sup>2</sup>,  
Isabela Souza dos Santos <sup>2</sup>, Nanashara Figueiredo Reis <sup>2</sup>, Arieli Bernardo Portugal <sup>3,4</sup>, João Luiz Mendes Wanderley <sup>3</sup>,  
André Borges Farias <sup>5,6</sup>, Nelilma Correia Romeiro <sup>6</sup> and Evanoel Crizanto de Lima <sup>2,\*</sup>

<sup>1</sup> Laboratório de Farmacologia e Bioquímica (LFBq), Departamento de Medicina Veterinária, Universidade de São Paulo Faculdade de Zootecnia e Engenharia de Alimentos, Av. Duque de Caxias Norte 225, Pirassununga 13635-900, SP, Brazil

<sup>2</sup> Laboratório de Catálise e Síntese de Substâncias Bioativas, Instituto Multidisciplinar de Química, CM UFRJ-Macaé, Universidade Federal do Rio de Janeiro, Macaé CEP 27971-525, RJ, Brazil

<sup>3</sup> Laboratório de Imunoparasitologia, Instituto de Ciências Médicas, Centro Multidisciplinar UFRJ, Macaé CEP 27979-000, RJ, Brazil

<sup>4</sup> Programa de Pós Graduação em Biociências e Biotecnologia, Universidade Estadual do Norte Fluminense, Campos dos Goytacazes CEP 28013-602, RJ, Brazil

<sup>5</sup> Unidad Académica de Yucatán, Instituto de Investigaciones en Matemáticas Aplicadas y en Sistemas, Universidad Nacional Autónoma de México, Mérida 97302, Yucatán, Mexico

<sup>6</sup> Integrated Laboratory of Scientific Computing (LICC), Federal University of Rio de Janeiro (UFRJ)—Campus Macaé, Aluizio Silva Gomes Avenue 50, Granjas Cavaleiros, Macaé 27930-560, RJ, Brazil

\* Correspondence: cmaquiaveli40@gmail.com (C.d.C.M.); edsilva@usp.br (E.R.d.S.); evanoel.crizanto@gmail.com (E.C.d.L.)



**Citation:** do Carmo Maquiaveli, C.; da Silva, E.R.; Hild de Jesus, B.; Oliveira Monteiro, C.E.; Rodrigues Navarro, T.; Pereira Branco, L.O.; Souza dos Santos, I.; Figueiredo Reis, N.; Portugal, A.B.; Mendes Wanderley, J.L.; et al. Design and Synthesis of New Anthranil Phenylhydrazides: Antileishmanial Activity and Structure–Activity Relationship. *Pharmaceuticals* **2023**, *16*, 1120. <https://doi.org/10.3390/ph16081120>

Academic Editor: Francisco Jaime Bezerra Mendonça Júnior

Received: 29 June 2023

Revised: 26 July 2023

Accepted: 7 August 2023

Published: 9 August 2023



**Copyright:** © 2023 by the authors. Licensee MDPI, Basel, Switzerland. This article is an open access article distributed under the terms and conditions of the Creative Commons Attribution (CC BY) license (<https://creativecommons.org/licenses/by/4.0/>).

**Abstract:** Leishmaniasis is a neglected tropical disease affecting millions of people worldwide. A centenary approach to antimonial-based drugs was first initiated with the synthesis of urea stibamine by Upendranath Brahmachari in 1922. The need for new drug development led to resistance toward antimonates. New drug development to treat leishmaniasis is urgently needed. In this way, searching for new substances with antileishmanial activity, we synthesized ten anthranil phenylhydrazide and three quinazolinone derivatives and evaluated them against promastigotes and the intracellular amastigotes of *Leishmania amazonensis*. Three compounds showed good activity against promastigotes 1b, 1d, and 1g, with IC<sub>50</sub> between 1 and 5 μM. These new phenylhydrazides were tested against *Leishmania* arginase, but they all failed to inhibit this parasite enzyme, as we have shown in a previous study. To explain the possible mechanism of action, we proposed the enzyme PTR1 as a new target for these compounds based on in silico analysis. In conclusion, the new anthranil hydrazide derivatives can be a promising scaffold for developing new substances against the protozoa parasite.

**Keywords:** *Leishmania*; polyamines; arginase; PTR1; anthranil hydrazides

## 1. Introduction

Leishmaniasis is a neglected tropical disease that affects 12 million people in the world; it is found in 98 countries, and an estimated one billion people are at risk of the disease [1]. The treatments for leishmaniasis disease are based on antimonial pentavalent as the first choice. This centenary approach-based drug was initiated first with the synthesis of urea stibamine by Upendranath Brahmachari in 1922 [2]. The urea stibamine significantly impacts the treatment of leishmaniasis, but the high toxicity led to the development of sodium stibogluconate in 1950 and N-methylglucamine antimonate (glucantime). However, antimonials have several limitations, including high toxicity, long treatment duration, and emerging resistance. This has prompted the exploration of alternative treatment options for leishmaniasis [3].

While antimonials have been the mainstay of leishmaniasis treatment for a century, alternative drugs such as miltefosine, amphotericin B, and pentamidine have emerged as effective options [1]. Amphotericin B, a polyene antifungal drug, interferes with membrane ergosterol, while pentamidine is involved in the polyamine biosynthesis pathway. These drugs are also highly toxic and unavailable for oral delivery [4].

Miltefosine is the first oral drug approved for leishmaniasis treatment. Miltefosine has shown promising efficacy against various forms of the disease, including visceral leishmaniasis (VL) and cutaneous leishmaniasis (CL) [5]. Despite being active against antimonial-resistant strains [5], resistance was described [6]. In Brazil, because of resistance to the miltefosine treatment in human visceral leishmaniasis, the drug is approved only to treat dogs infected by *Leishmania* [7].

Researchers continue to explore old and new targets for rational drug design. For example, a second line of alternative treatment was carried out using allopurinol, which blocks the de novo synthesis of purines [8–10]. A world effort to develop new drugs against this neglected tropical disease involves low private and public investments, mainly at the academic level. Repurposing was also explored with marbofloxacin, a fluoroquinolone that inhibits the topoisomerase (DNA gyrase) and tamoxifen, an antitumoral agent [11,12].

The polyamine biosynthesis pathway [13] is a promising route to drug development targeting arginase [14] and ornithine decarboxylase (ODC) [15]. We previously explored the synthesis of several scaffolds, such as cinnamic acid, pyrazolopyrimidines, and phenylhydrazides, using *Leishmania* arginase as a target. They all showed selective arginase inhibition and good activity against parasites, inspiring a new scaffold of anthranil phenylhydrazides [16]. Until now, no other hydrazides with leishmanicidal activity have been described in the literature, except for those previously published by our group [16], for which its structure was based on eflornithine, an inhibitor of the ODC enzyme. This study tests 13 structural hydrazides related to the previously prepared  $\alpha,\alpha$ -difluoromethylhydrazide as a prototype for designing anthranil phenylhydrazides using molecular simplification. These anthranil phenylhydrazides showed better activity against *Leishmania amazonensis* promastigotes than the previous  $\alpha,\alpha$ -difluoromethylhydrazide series [16].

## 2. Results and Discussion

### 2.1. Chemistry

Anthranil hydrazides were carried out with isatoic anhydride and phenylhydrazine under reflux in ethanol for 2 h [17]. In cases where phenylhydrazine is available in salt form, NaOH was used to obtain the free nucleophile. Posteriorly, hydrazides 1a, 1d, and 1g were cyclized, furnishing respective quinazolin-4(3H)-ones 2a, 2b, and 2c using acetyl chloride and CH<sub>3</sub>CN as the solvent at room temperature for 3 h. The reaction with acetic anhydride was also conducted, but the reaction times were higher, ~6–9 h.

### 2.2. Planning of Anthranil Hydrazides Series

Based on our previous results with the  $\alpha,\alpha$ -difluorophenyl hydrazide series, new compounds were designed from the phenylhydrazide previously characterized as a pharmacophoric group for antileishmanial activity [16]. Figure 1 shows the phenylhydrazide and aminophenyl groups in the compounds using a molecular simplification approach.

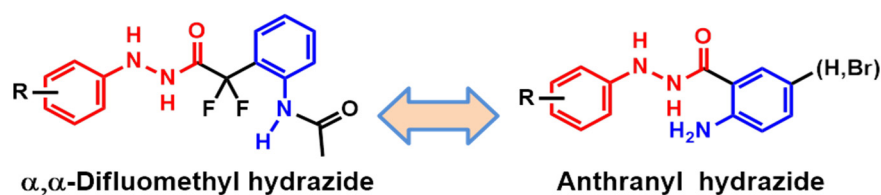
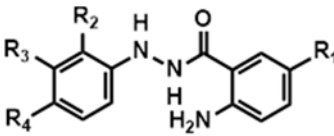
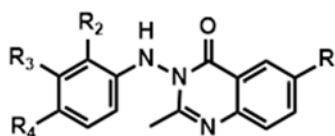


Figure 1. Anthranil hydrazides designed from  $\alpha,\alpha$ -difluoromethylhydrazide.

### 2.3. Activity in Promastigotes and Intracellular Amastigotes

The study of  $\alpha$ - $\alpha$ -difluorophenyl hydrazides compounds revealed the phenylhydrazide group as a new pharmacophoric group against *L. amazonensis* [16]. Another series of anthranil hydrazide compounds were planned as potential agents against Leishmania. In a screening of *L. amazonensis* promastigote cultures, all compounds showed inhibition above 50% at 100  $\mu$ M. We screened at 10  $\mu$ M and selected four compounds to determine the  $IC_{50}$ . However, **1e** showed myelotoxicity in an animal model [17], and we did not determine the  $IC_{50}$ . The best result in the trial at 10  $\mu$ M was observed for compound **1g**, which showed 97% growth inhibition with an  $IC_{50}$  of 1.3  $\mu$ M (Table 1).

**Table 1.** Screening of compounds and comparison of  $IC_{50}$  of compounds showed more significant promastigote growth inhibition at 10  $\mu$ M.

						
	R <sub>1</sub>	R <sub>2</sub>	R <sub>3</sub>	R <sub>4</sub>	Inhibition at 10 $\mu$ M (%)	$IC_{50}$ ( $\mu$ M) (95% CI)
<b>1a</b>	H	H	H	H	41.3	>10
<b>1b</b>	Br	H	H	H	67.7	4.2 (3.460–5.038)
<b>1c</b>	H	Br	H	H	30.0	>10
<b>1d</b>	H	H	H	Br	55.2	5.3 (4.963–5.670)
<b>1e</b>	H	H	H	Cl	59.2	<10
<b>1f</b>	H	H	H	F	12.8	>10
<b>1g</b>	Br	H	H	Br	97.9	1.3 (1.177–1.411)
<b>1h</b>	H	CH <sub>3</sub>	H	H	4.4	>10
<b>1i</b>	H	H	CH <sub>3</sub>	H	nd	~20
<b>1j</b>	H	H	H	CH <sub>3</sub>	nd	~20
<b>2a</b>	H	H	H	H	inactive	-
<b>2b</b>	H	H	H	Br	inactive	-
<b>2c</b>	Br	H	H	Br	inactive	-

CI, confidence interval; nd, not determined.

Thus, we determined the  $IC_{50}$  for compounds **1b**, **1d**, and **1g** (Figure 2). Compound **1g** was the most potent, with an  $IC_{50}$  of 1.3  $\mu$ M. An ANOVA test was applied, followed by Tukey's post hoc test, which indicated that **1d** differs significantly from **1b** ( $p < 0.05$ ) and **1g** differs from **1d** and **1b** ( $p < 0.001$ ).

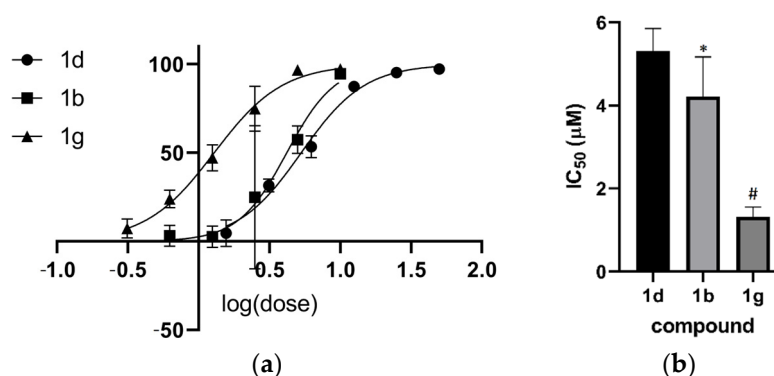


**Figure 2.** Comparison of promastigote activity of the anthranil hydrazides series. (a) Curve log (dose) response; (b)  $IC_{50}$  comparison. #  $p < 0.001$  vs. **1d** and **1b**; \*  $p < 0.05$  vs. **1d**.

Despite the good activity against *L. amazonensis* promastigotes, the compounds failed against intracellular amastigotes using peritoneal murine macrophage (data not shown). *Leishmania* spp. use several approaches for resistance against drugs [3]. One is the ABC transporter MRPA (PGPA) in antimony resistance described for *Leishmania infantum* [18]. The PRP1, an ABC transporter superfamily member, was correlated with pentamidine resistance in *Leishmania major* [19]. A new study must be performed to understand why the hydrazide compounds were inactive against intracellular amastigotes.

#### 2.4. Structure–Activity Relationship Analysis of the Anthranil Hydrazides Series

By comparing the  $IC_{50}$  in promastigote culture, it can be inferred that halogenation with chlorine or bromine in the p-phenyl (R4) position increases antileishmanial activity. The leishmanial inhibition growth was also observed with bromine at position R1 (compound **1b**,  $IC_{50} = 4.2 \mu M$ ), and higher inhibition was observed with bromine at position R1 and R4 in compound **1g** ( $IC_{50} = 1.3 \mu M$ ).

The promastigote culture test results also showed that the anthranil hydrazide series was superior to the  $\alpha$ - $\alpha$ -difluorohydrazides compounds. With the culture result obtained for the  $\alpha$ - $\alpha$ -difluorohydrazides [16] compound series, we identified the pharmacophoric phenylhydrazide group and produced a new series of compounds. In the present study, the insertion of bromine into the phenyl groups at positions R1 and R4 (Figure 3) increased the growth-inhibitory potency of the promastigote forms by about 10-fold. The new compound **1g** showed an  $IC_{50} = 1.3 \mu M$ , while compound **4** showed an  $IC_{50}$  of  $12.7 \mu M$  [16].

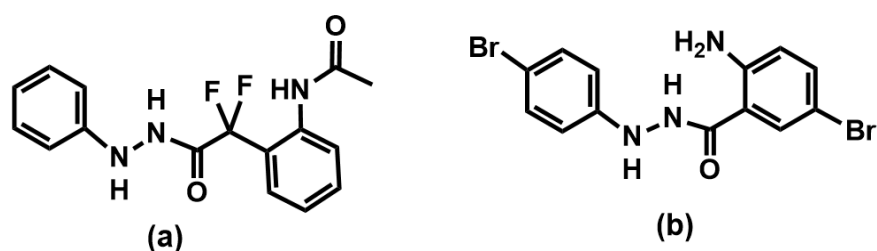


**Figure 3.** The structure of  $\alpha$ - $\alpha$ -difluorohydrazides and anthranil phenylhydrazide: (a) compound **4** [16] and (b) compound **1g**.

The derived compounds **2a**, **2b**, and **2c** were inactive, showing that the scaffold used in compounds **1(a–j)** is essential for the activity against *L. amazonensis*.

#### 2.5. Mechanism of Antileishmanial Activity

Based on previous results with phenylhydrazides [16] that inhibit *Leishmania* arginase, we tested the possible enzyme inhibition in vitro. All anthranil phenylhydrazides failed as *Leishmania* arginase inhibitors, and to propose a new method of parasite killing, we performed target fishing as follows.

#### 2.6. Target Fishing for Anthranil Phenylhydrazides

A target-fishing approach was performed using chemogenomics to provide new targets for phenylhydrazide inhibitors. Several studies have demonstrated the ability of this approach to predict promising targets [20,21]. Thus, some targets, including arginase, were predicted as potential targets for inhibitors (Table S1). Unfortunately, the results in this work revealed that the synthesized inhibitors had no activity on arginase, leading to the search for new targets for *L. amazonensis*. Due to the absence or lack of information about *L. amazonensis* in the database, it was impossible to directly predict a target. However, the target-fishing predictions by chemogenomics suggested pteridine reductase 1 (PTR1) from *L. major* as a possible target. An alignment (Figure S1) was performed on the primary sequence of PTR1 to search for a homologous protein for *L. amazonensis*, indicating aldoketoreductase (GenBank AAB61214.1) with 100% query cover and 91.67% identity.

Pteridine reductase is an NADPH-dependent reductase that catalyzes the reduction in folate and biopterin into their biologically active forms, tetrahydrofolate and tetrahydrobiopterin, respectively [22]. It is the only enzyme to perform this reduction in *Leishmania*, proving essential for their in vivo growth by gene knockout studies [23]. Furthermore, *Leishmania* is auxotrophic for folate and other pterins required in critical pathways related to nucleic acids and protein synthesis [24,25]. Therefore, the drug development of new inhibitors for PTR1 would be a promising strategy for the treatment of leishmaniasis [26–28]. Although target fishing provides significant results on possible molecular targets, this technique depends on molecular scaffolds in the database, often with sparse data for specific organisms. Thus, molecular docking was performed to obtain the theoretical binding mode of the designed compounds with PTR1 from *L. amazonensis*. Despite the PTR1 binding site from *L. amazonensis* being very similar to *L. major* (RMSD of 1.30 Å over 264 residues), 24 amino acids are not conserved (Figure S1). Of these 24 residues, only two, A229 and Y240, are within 5 Å of the inhibitor methotrexate. The catalytic center is formed by  $\beta 1$ ,  $\beta 4$ ,  $\beta 5$ , and  $\beta 6$ , located in the C-terminal regions,  $\alpha 1$  and  $\alpha 5$  of the N-terminal, and a loop between  $\beta 6$  and  $\alpha 6$  [29]. The results showed that compound **1g** could interact with two residues of the catalytic triad (Y193 and D180) by hydrogen bonding. Besides that,  $\pi$ - $\pi$  stacked interactions with F113 and the cofactor were also observed (Figure 4). Notably, the other molecules, in general, presented a similar putative binding mode (Figures S2 and S3), indicating that this molecular scaffold may be relevant to the drug design of new candidates to treat leishmaniasis. Similarity with the crystallized co-inhibitor methotrexate was also observed (Figure S4), mainly concerning the interaction with the catalytic residue Y193 (Y194 in PTR1 from *L. major*). Gourley et al. described PTR1's mechanism of action, involving hydrogen bonds between Y194 and a nucleophilic center of the substrate, bound to stabilize the transition state to provide the proton transferred in the reaction [29]. Therefore, the observed interactions support the hypothesis of PTR1 as a target of the studied compounds.

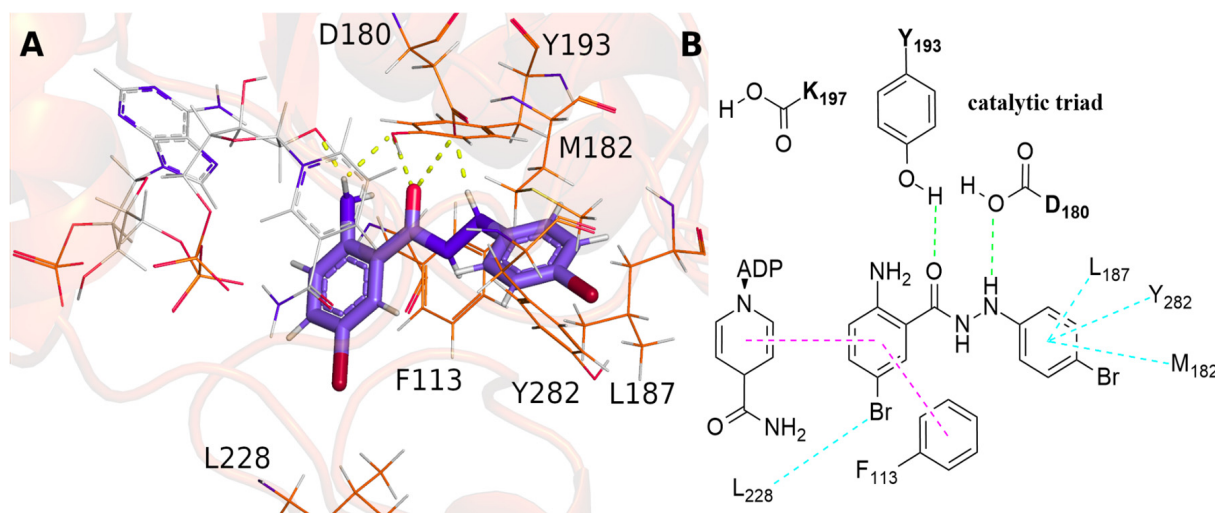


**Figure 4.** (A) Putative binding pose of inhibitor **1g** with PTR1 as suggested by molecular docking. (B) Scheme with the main interactions carried out in the active site. Hydrogen bond,  $\pi$ -stacked, and alkyl/ $\pi$ -alkyl interactions are represented by green, magenta, and cyan dashed lines, respectively.

Further studies need to be conducted to validate the molecular docking hypothesis into PTR1 inhibition, such as enzymatic binding assays. However, PTR1 is a recognized target for leishmanicidal drug design [26,30] since it provides enough folate to guarantee the parasite's survival [31]. Taken together, this preliminary study, associated with the inhibition in promastigote cells and the prediction by chemogenomics, is a promising molecular target for developing new inhibitors based on the phenylhydrazide scaffold.

### 3. Materials and Methods

#### 3.1. Chemicals

The M199 medium was supplemented with 10% fetal bovine serum, 5 ppm of hemin, 50 µg/mL streptomycin, and 100 U penicillin. Hanks Balanced Salt Solution (GIBCO® HBSS) was purchased from Thermo Life technologies, and MTT 3-(4,5-dimethylthiazol-2-yl)-2,5-diphenyl tetrazolium bromide was purchased from Sigma.

#### 3.2. Synthesis

The anthranil hydrazides were prepared using the experimental procedure previously reported, in which improvements were made compared to the literature [17]. Quinazolin-4(3H)-ones **2a**, **2b**, and **2c** were prepared from respective phenyl hydrazides (1.89 mmol), using acetyl chloride (9.45 mmol) and CH<sub>3</sub>CN (2.5 mL) as solvent at room temperature. TLC accomplished reactions by 3 h, and after this period, cold water was added to the reaction mixture. The solid was filtered, having sufficient purity to be tested posteriorly.

##### 3.2.1. Synthesis of 2-amino-5-bromo-N'-phenylbenzohydrazide (**1b**)

Yellow solid, 55% yield. GC-MS: *m/z* 307 (34%), *m/z* 305 (34%), *m/z* 200 (100%), *m/z* 198 (99%), *m/z* 170 (21%). ESI-MS(+) C<sub>13</sub>H<sub>12</sub>BrN<sub>3</sub>NaO: *m/z* 328.0055.

##### 3.2.2. Synthesis of 2-amino-N'-(2-bromophenyl)benzohydrazide (**1c**)

Pale solid, 95% yield. GC-MS: *m/z* 307 (15%), *m/z* 305 (15%), *m/z* 120 (100%), *m/z* 92 (22%). ESI-MS(+) C<sub>13</sub>H<sub>13</sub>BrN<sub>3</sub>O: *m/z* 306.0237; C<sub>13</sub>H<sub>12</sub>BrN<sub>3</sub>NaO: *m/z* 328.0053.

NMR <sup>1</sup>H (MeOD, 400 MHz, δ): 7.62 (d, 1H, *J* = 7.9 Hz), 7.44 (d, 1H, *J* = 7.9 Hz), 7.25 (t, 1H, *J* = 8 Hz), 7.21 (t, 1H, *J* = 8 Hz), 6.94 (d, 1H, *J* = 8.2 Hz), 6.78 (d, 1H, *J* = 8.3 Hz), 6.73 (t, 1H, *J* = 7.8 Hz), 6.67 (t, 1H, *J* = 7.8 Hz).

##### 3.2.3. Synthesis of 2-amino-5-bromo-N'-(4-bromophenyl) benzohydrazide (**1g**)

Yellow solid, 52% yield. GC-MS: *m/z* 385 (22%), *m/z* 200 (98%), *m/z* 198 (100%), *m/z* 172 (16%), *m/z* 170 (16%). ESI-MS(+) C<sub>13</sub>H<sub>11</sub>Br<sub>2</sub>N<sub>3</sub>NaO: *m/z* 405.9156.

NMR <sup>1</sup>H (DMSO-d<sub>6</sub>, 400 MHz, δ): 10.21 (s, 1H, NH), 7.99 (s, 1H, NH), 7.80 (d, 1H, *J* = 2.3 Hz), 7.31–7.28 (l, 3H), 6.74–6.70 (l, 3H), 6.54 (s, 2H, NH<sub>2</sub>).

##### 3.2.4. Synthesis of 2-amino-N'-(m-tolyl)benzohydrazide (**1i**)

Pale solid, 88% yield. GC-MS: *m/z* 241 (31%), *m/z* 121 (11%), *m/z* 120 (100%), *m/z* 92 (21%). ESI-MS(+) C<sub>14</sub>H<sub>15</sub>N<sub>3</sub>NaO: *m/z* 264.1109.

NMR <sup>1</sup>H (MeOD, 400 MHz, δ): 7.58 (d, 1H, *J* = 11.9 Hz), 7.22 (t, 1H, *J* = 7.8 Hz), 7.06 (t, 1H, *J* = 7.8 Hz), 6.78 (d, 1H, *J* = 8.2 Hz), 6.71–6.63 (m, 4H), 2.26 (s, 3H).

##### 3.2.5. Synthesis of 2-amino-N'-(p-tolyl)benzohydrazide (**1j**)

Pale solid, 88% yield. GC-MS: *m/z* 241 (34%), *m/z* 121 (11%), *m/z* 120 (100%), *m/z* 106 (7%), *m/z* 92 (20%). ESI-MS(+) C<sub>14</sub>H<sub>15</sub>N<sub>3</sub>NaO: *m/z* 264.1110.

NMR <sup>1</sup>H (MeOD, 400 MHz, δ): 7.57 (d, 1H, *J* = 7.9 Hz), 7.22 (t, 1H, *J* = 7.7 Hz), 7.01 (d, 2H, *J* = 8.0 Hz), 6.80–6.77 (m, 3H), 6.66 (t, 1H, *J* = 7.9 Hz), 2.23 (s, 3H).

##### 3.2.6. Synthesis of 2-methyl-3-(phenylamino)quinazolin-4(3H)-one (**2a**)

Pale solid, 85% yield. GC-MS: *m/z* 251 (100%), *m/z* 236 (13%), *m/z* 146 (30%), *m/z* 117 (13%).

##### 3.2.7. 3-((4-bromophenyl)amino)-2-methylquinazolin-4(3H)-one (**2b**)

White solid, 51% yield. GC-MS: *m/z* 331 (97%), *m/z* 329 (100%), *m/z* 172 (41%), *m/z* 170 (42%), *m/z* 146 (65%).

### 3.2.8. Synthesis of 6-bromo-3-((4-bromophenyl)amino)-2-methylquinazolin-4(3H)-one (2c)

Yellow solid, 79% yield. GC-MS:  $m/z$  411 (50%),  $m/z$  409 (100%),  $m/z$  172 (29%),  $m/z$  170 (34%).

### 3.3. Promastigotes Test

*L. amazonensis* (MHOM/BR/1973/M2269 strain) was used in this study. Promastigotes were grown in an M199 medium supplemented with 10% fetal bovine serum, 5 ppm of hemin, 50  $\mu\text{g}/\text{mL}$  streptomycin, and 100 U penicillin until they reached the stationary phase. Initially,  $5.0 \times 10^5$  cells were incubated with or without the compounds at variable concentrations. Amphotericin B was used as a positive control. The effect was available 24 h, 48 h, and 72 h after incubation with test compounds. The test culture was washed twice with 1 mL of Hanks Balanced Salt Solution (GIBCO<sup>®</sup> HBSS). After that, the cultures were incubated overnight with dye MTT added to the culture medium at a final concentration of 0.5 mg/mL. The formazan crystals were dissolved with 200  $\mu\text{L}$  of DMSO, and the formazan concentration was determined using the Epoch 2 Microplate Spectrophotometer (Biotech, Instruments, Winooski, VT, USA) at 570 nm.  $\text{IC}_{50}$  values were estimated using a sigmoidal model (Log  $\text{IC}_{50}$ ) in a normalized variable slope in the GraphPad Prism software (version 9.5 for Windows, San Diego, CA, USA). Two independent assays were performed in triplicate [32].

### 3.4. Arginase Assay

For the compound test against *L. amazonensis* arginase (ARG-L), the recombinant was obtained by overexpressing the enzyme in *Escherichia coli*, followed by purification as described previously [33]. Briefly, an *E. coli* culture containing the gene from *L. amazonensis* arginase culture was grown until  $\text{DO}_{600} = 0.6$ . Then, the enzyme production was induced with 1 mM IPTG in 1 L of SOB medium enriched with 10 mM of  $\text{MnSO}_4$ . After 3 h of induction, the enzyme was purified [33]. An inhibition assay was conducted by incubating the arginase with the test compounds at 100  $\mu\text{M}$  using 50 mM CHES buffer and 50 mM L-arginine at pH 9.5 for 15 min [14]. The negative control was performed without the inhibitor, and quercetin was used as a positive inhibition control [14]. The arginase activity was then measured by quantifying urea by the Berthelot method [34].

### 3.5. Target Fishing with Chemogenomics

To predict the compound targets, a chemogenomics approach was used. First, the chemical structures of the compounds were drawn in ChemDrawn v.12.0.2 and prepared with ChemAxon Standardizer (v.16.5.2.0, 2016, <http://www.chemaxon.com>, accessed on 30 May 2023), in which the SMILE (Simplified Molecular Input Line Entry Specification) notation was generated and standardized, i.e., aromaticity, charges, and tautomers were assigned. Target predictions were created with Pidgin software v.2 [35,36] using predict\_binary.py with 0.5 predicted true positive rate. The software compared the structural similarity between our compounds and molecules using Morgan fingerprints with the biological activity described in the databases and included in the predictive models' construction. Thus, the molecules present in the database with known molecular targets were compared with the present work, and the results were filtered to obtain only the targets with similarity above the cutoff value. Pteridine reductase 1, from *Leishmania major*, was selected to perform a search for homologous proteins on the NCBI server using Blastp [37]. The alignment of the amino acid sequences was performed on the Praline server [38]. The sequence and structure of Pteridine reductase 1, from *L. amazonensis*, were obtained in Uniprot under the code O09352.

### 3.6. Molecular Docking Studies

Since there are no available experimental structures of *L. amazonensis* PTR1 in the databases, the AlphaFold [39,40] server was used to obtain its three-dimensional structure. To validate the parameters for docking studies, a redocking approach was applied with

GOLD [41] (Genetic Optimization for Ligand Docking) v. 2022.3.0 with the 3D structure of PTR1 from *L. major*, PDB code 1E7W [30], with a resolution of 1.75 Å. The water molecules and cofactors interacting with the inhibitor methotrexate (MTX) were maintained. In this study, all docking-scoring functions with a search radius of 10 and 20 Å related to amino acid residues S111, Y194, and Y191 as references were used to estimate the best parameters. Thus, the goldscore function with 10 Å of search radius around Y191 with flexible residues F113 and Y194 reproduced the best superposition between co-crystallized methotrexate (MTX) and the top docking solution. Twenty runs of the genetic algorithm were performed for each molecule. The cofactor coordinate in the *L. amazonensis* PTR1 structure was obtained by structural alignment with the *L. major* PTR1 crystal structure. Model validation metrics were obtained from the Ramachandran plot on the Procheck server [42] and the Z-score and local energy quality on the Prosa-web server (Figures S5–S7) [43,44].

The inhibitors were built with Avogadro v. 1.93.0 [45], and the energy was minimized using the PM3 semi-empirical method available in the Gaussian 09 package. All docking poses and interaction analyses were performed using Pymol v. 2.4.0a0 [46] and Discovery Studio 2016 Visualizer [47].

#### 4. Conclusions

The new anthranil phenylhydrazide showed better activity against *L. amazonensis* promastigotes when compared to  $\alpha$ - $\alpha$ -difluorohydrazides. Compound **1g** (IC<sub>50</sub> = 1.3  $\mu$ M) was 10-fold more potent than compound **4** (IC<sub>50</sub> = 12.7  $\mu$ M), an  $\alpha$ - $\alpha$ -difluorohydrazide that was characterized previously [16]. The bromine at positions R1 and R4 is better than only bromine at R1 (**1b**) or only at R4 (**1d**). Target fishing for anthranil phenylhydrazides indicates the possible mechanism of action for these compounds by inhibiting the parasite enzyme PTR1. The scaffold of anthranil phenylhydrazide of series 1 is essential for antileishmanial activity. Thus, we conclude that these compounds are promising for developing new substances against *Leishmania*.

**Supplementary Materials:** The following supporting information can be downloaded at: <https://www.mdpi.com/article/10.3390/ph16081120/s1>, Figure S1: Alignment between PTR1 of *L. amazonensis* and *L. major*; Figure S2: (A) Overlay of Putative binding pose. Docking analysis of inhibitors (B) 1a (C) 1d and (D) 1e. Interactions are colored by type: hydrogen bond, van der Waals, alkyl, Pi-stacked, halogen, unfavorable donor-donor, and Pi-anion/cation are shown by colors green, light green, light pink, pink, cyan, red, and gold, respectively; Figure S3: (A) Docking analysis of inhibitors 1f (B) 1j (C) 1c and (D) 1g. Interactions are colored by type: hydrogen bond, van der Waals, alkyl, Pi-stacked, halogen, unfavorable donor-donor, and Pi-anion/cation are shown by colors green, light green, light pink, pink, cyan, red, and gold, respectively; Figure S4: (A) Structural alignment between PTR1 from *L. major* (yellow) and *L. amazonensis* (orange). (B) Comparison between docking pose of inhibitor 1g and methotrexate co-crystallized in PTR1; Figure S5: Ramachandran plot of PTR1 model from *L. amazonensis* obtained in AlphaFold; Figure S6: Predicted error of PTR1 model from *L. amazonensis* obtained in AlphaFold; Figure S7: (A) Comparison of the z-score of our model against all protein chains in PDB determined by X-ray crystallography (light blue) or NMR spectroscopy (dark blue). (B) Local model quality observed by residue energies averaged in two windows, size 10 (light green) and 40 (green); Table S1. Targets predicted by chemogenomics.

**Author Contributions:** Conceptualization, C.d.C.M., A.B.F., N.C.R. and E.C.d.L.; formal analysis, C.d.C.M., E.R.d.S., J.L.M.W. and A.B.F.; funding acquisition, C.d.C.M., E.R.d.S. and E.C.d.L.; investigation, E.R.d.S., B.H.d.J., C.E.O.M., T.R.N., L.O.P.B., I.S.d.S., N.F.R., A.B.P., J.L.M.W., A.B.F. and N.C.R.; methodology, C.d.C.M., E.R.d.S., A.B.F., N.C.R. and E.C.d.L.; project administration, E.R.d.S. and E.C.d.L.; resources, E.R.d.S. and E.C.d.L.; supervision, C.d.C.M., E.R.d.S. and E.C.d.L.; writing—original draft, C.d.C.M., E.R.d.S., A.B.F., N.C.R. and E.C.d.L.; writing—review and editing, C.d.C.M., E.R.d.S., A.B.F. and E.C.d.L. All authors have read and agreed to the published version of the manuscript.

**Funding:** This research was funded by grant #19/23769-4, São Paulo Research Foundation (FAPESP), grant SEI-260003/001219/2020 and grant E-26/010.101122/2018, Fundação Carlos Chagas Filho de

Amparo à Pesquisa do Estado do Rio de Janeiro (FAPERJ), and this study was financed in part by the Coordenação de Aperfeiçoamento de Pessoal de Nível Superior–Brasil (CAPES)–Finance Code 001.

**Institutional Review Board Statement:** The animal study protocol was approved by the Institutional Ethics Committee of Faculdade de Zootecnia e Engenharia de Alimentos da Universidade de São Paulo—FZEA/USP (CEUA/FZEA), protocol CEUA n° 3086190918, 01/23/2019 for studies involving animals.

**Informed Consent Statement:** Not applicable.

**Data Availability Statement:** Data is contained within the article and supplementary material.

**Conflicts of Interest:** The authors declare no conflict of interest.

## References

1. WHO | Leishmaniasis. WHO. 2019. Available online: <https://www.who.int/leishmaniasis/en/> (accessed on 27 June 2019).
2. Saha, P.; Chaudhury, A.; Maji, A.K. Sir U.N. Brahmachari and his battle against Kala-Azar. *Trop. Parasitol.* **2021**, *11*, 89. [[CrossRef](#)] [[PubMed](#)]
3. Ponte-Sucre, A.; Gamarro, F.; Dujardin, J.-C.; Barrett, M.P.; López-Vélez, R.; García-Hernández, R.; Pountain, A.W.; Mwenechanya, R.; Papadopoulou, B. Drug resistance and treatment failure in leishmaniasis: A 21st century challenge. *PLoS Neglected Trop. Dis.* **2017**, *11*, e0006052. [[CrossRef](#)]
4. Basselin, M.; Badet-Denisot, M.-A.; Lawrence, O.; Robert-Gero, M. Effects of Pentamidine on Polyamine Level and Biosynthesis in Wild-Type, Pentamidine-Treated, and Pentamidine-Resistant Leishmania. *Exp. Parasitol.* **1997**, *85*, 274–282. [[CrossRef](#)]
5. Monge-Maillo, B.; Lopez-Velez, R. Miltefosine for Visceral and Cutaneous Leishmaniasis: Drug Characteristics and Evidence-Based Treatment Recommendations. *Clin. Infect. Dis.* **2015**, *60*, 1398–1404. [[CrossRef](#)] [[PubMed](#)]
6. Rai, K.; Cuyppers, B.; Bhattarai, N.R.; Uranw, S.; Berg, M.; Ostyn, B.; Dujardin, J.C.; Rijal, S.; Vanaerschot, M. Relapse after treatment with Miltefosine for visceral Leishmaniasis is associated with increased infectivity of the infecting Leishmania donovani strain. *mBio* **2013**, *4*, e00611-13. [[CrossRef](#)] [[PubMed](#)]
7. Dos Santos Nogueira, F.; Avino, V.C.; Galvis-Ovallos, F.; Pereira-Chioccola, V.L.; Moreira, M.A.B.; Romariz, A.P.P.L.; Molla, L.M.; Menz, I. Use of miltefosine to treat canine visceral leishmaniasis caused by Leishmania infantum in Brazil. *Parasites Vectors* **2019**, *12*, 79. [[CrossRef](#)]
8. Ginel, P.J.; Lucena, R.; López, R.; Molleda, J.M. Use of allopurinol for maintenance of remission in dogs with leishmaniasis. *J. Small Anim. Pract.* **1998**, *39*, 271–274. [[CrossRef](#)]
9. Manna, L.; Vitale, F.; Reale, S.; Picillo, E.; Neglia, G.; Vescio, F.; Gravino, A.E. Study of efficacy of miltefosine and allopurinol in dogs with leishmaniosis. *Vet. J.* **2009**, *182*, 441–445. [[CrossRef](#)]
10. Manna, L.; Corso, R.; Galiero, G.; Cerrone, A.; Muzj, P.; Gravino, A.E. Long-term follow-up of dogs with leishmaniosis treated with meglumine antimoniate plus allopurinol versus miltefosine plus allopurinol. *Parasites Vectors* **2015**, *8*, 289. [[CrossRef](#)]
11. Trinconi, C.T.; Reimão, J.Q.; Bonano, V.I.; Espada, C.R.; Miguel, D.C.; Yokoyama-Yasunaka, J.K.U.; Uliana, S.R.B. Topical tamoxifen in the therapy of cutaneous leishmaniasis. *Parasitology* **2018**, *145*, 490–496. [[CrossRef](#)]
12. Pineda, C.; Aguilera-Tejero, E.; Morales, M.C.; Belinchon-Lorenzo, S.; Gomez-Nieto, L.C.; Garcia, P.; Martinez-Moreno, J.M.; Rodriguez-Ortiz, M.E.; Lopez, I. Treatment of canine leishmaniasis with marbofloxacin in dogs with renal disease. *PLoS ONE* **2017**, *12*, e0185981. [[CrossRef](#)] [[PubMed](#)]
13. Bocedi, A.; Dawood, K.F.; Fabrini, R.; Federici, G.; Gradoni, L.; Pedersen, J.Z.; Ricci, G. Trypanothione efficiently intercepts nitric oxide as a harmless iron complex in trypanosomatid parasites. *FASEB J.* **2010**, *24*, 1035–1042. [[CrossRef](#)] [[PubMed](#)]
14. Da Silva, E.R.; Maquiaveli, C.D.C.; Magalhães, P.P. The leishmanicidal flavonols quercetin and quercitrin target Leishmania (Leishmania) amazonensis arginase. *Exp. Parasitol.* **2012**, *130*, 183–188. [[CrossRef](#)]
15. Jiang, Y.; Roberts, S.C.; Jardim, A.; Carter, N.S.; Shih, S.; Ariyanayagam, M.; Fairlamb, A.H.; Ullman, B. Ornithine decarboxylase gene deletion mutants of Leishmania donovani. *J. Biol. Chem.* **1999**, *274*, 3781–3788. [[CrossRef](#)] [[PubMed](#)]
16. de Lima, E.C.; Castelo-Branco, F.S.; Maquiaveli, C.C.; Farias, A.B.; Rennó, M.N.; Boechat, N.; Silva, E.R. Phenylhydrazides as inhibitors of Leishmania amazonensis arginase and antileishmanial activity. *Bioorganic Med. Chem.* **2019**, *27*, 3853–3859. [[CrossRef](#)]
17. Paiva, J.P.B.; Cordeiro, M.S.; França, P.R.C.; Branco, L.O.P.; Santos, I.S.; Reis, N.F.; Pimentel, P.P.; Giorno, T.B.S.; Lima, E.C.; Fernandes, P.D. Phenylbenzohydrazides Obtained from Isatoic Anhydride Present Anti-Inflammatory Activity In Vivo and In Vitro. *Biomolecules* **2022**, *12*, 1901. [[CrossRef](#)]
18. El Fadili, K.; Messier, N.; Leprohon, P.; Roy, G.; Guimond, C.; Trudel, N.; Saravia, N.G.; Papadopoulou, B.; Légaré, D.; Ouellette, M. Role of the ABC transporter MRPA (PGPA) in antimony resistance in Leishmania infantum axenic and intracellular amastigotes. *Antimicrob. Agents Chemother.* **2005**, *49*, 1988–1993. [[CrossRef](#)]
19. Coelho, A.C.; Beverley, S.M.; Cotrim, P.C. Functional genetic identification of PRP1, an ABC transporter superfamily member conferring pentamidine resistance in Leishmania major. *Mol. Biochem. Parasitol.* **2003**, *130*, 83–90. [[CrossRef](#)]
20. Maghsoudi, S.; Taghavi Shahraki, B.; Rameh, F.; Nazarabi, M.; Fatahi, Y.; Akhavan, O.; Rabiee, M.; Mostafavi, E.; Lima, E.C.; Saeb, M.R.; et al. A review on computer-aided chemogenomics and drug repositioning for rational COVID-19 drug discovery. *Chem. Biol. Drug Des.* **2022**, *100*, 699–721. [[CrossRef](#)]

21. Jones, L.H.; Bunnage, M.E. Applications of chemogenomic library screening in drug discovery. *Nat. Rev. Drug Discov.* **2017**, *16*, 285–296. [[CrossRef](#)]
22. Nare, B.; Garraway, L.A.; Vickers, T.J.; Beverley, S.M. PTR1-dependent synthesis of tetrahydrobiopterin contributes to oxidant susceptibility in the trypanosomatid protozoan parasite *Leishmania major*. *Curr. Genet.* **2009**, *55*, 287. [[CrossRef](#)] [[PubMed](#)]
23. Nare, B.; Hardy, L.W.; Beverley, S.M. The roles of pteridine reductase 1 and dihydrofolate reductase-thymidylate synthase in pteridine metabolism in the protozoan parasite *Leishmania major*. *J. Biol. Chem.* **1997**, *272*, 13883–13891. [[CrossRef](#)] [[PubMed](#)]
24. Opperdoes, F.R.; Coombs, G.H. Metabolism of *Leishmania*: Proven and predicted. *Trends Parasitol.* **2007**, *23*, 149–158. [[CrossRef](#)]
25. Ouellette, M.; Drummelsmith, J.; El Fadili, A.; Kündig, C.; Richard, D.; Roy, G. Pterin transport and metabolism in *Leishmania* and related trypanosomatid parasites. *Int. J. Parasitol.* **2002**, *32*, 385–398. [[CrossRef](#)] [[PubMed](#)]
26. Das Neves, G.M.H.; Kagami, L.P.; Gonçalves, I.L.; Eifler-Lima, V.L. Targeting pteridine reductase 1 and dihydrofolate reductase: The old is a new trend for leishmaniasis drug discovery. *Futur. Med. Chem.* **2019**, *11*, 2107–2130. [[CrossRef](#)] [[PubMed](#)]
27. de Souza Moreira, D.; Ferreira, R.F.; Murta, S.M.F. Molecular characterization and functional analysis of pteridine reductase in wild-type and antimony-resistant *Leishmania* lines. *Exp. Parasitol.* **2016**, *160*, 60–66. [[CrossRef](#)] [[PubMed](#)]
28. Leite, F.H.A.; Froes, T.Q.; da Silva, S.G.; de Souza, E.I.M.; Vital-Fujii, D.G.; Trossini, G.H.G.; Pita, S.S.D.R.; Castilho, M.S. An integrated approach towards the discovery of novel non-nucleoside *Leishmania major* pteridine reductase 1 inhibitors. *Eur. J. Med. Chem.* **2017**, *132*, 322–332. [[CrossRef](#)] [[PubMed](#)]
29. Gourley, D.G.; Schüttelkopf, A.W.; Leonard, G.A.; Luba, J.; Hardy, L.W.; Beverley, S.M.; Hunter, W.N. Pteridine reductase mechanism correlates pterin metabolism with drug resistance in trypanosomatid parasites. *Nat. Struct. Biol.* **2001**, *8*, 521–525. [[CrossRef](#)]
30. Vickers, T.J.; Beverley, S.M. Folate metabolic pathways in *Leishmania*. *Essays Biochem.* **2011**, *51*, 63–80. [[CrossRef](#)]
31. Nare, B.; Luba, J.; Hardy, L.W.; Beverley, S. New approaches to *Leishmania* chemotherapy: Pteridine reductase 1 (PTR1) as a target and modulator of antifolate sensitivity. *Parasitology* **1997**, *114*, 101–110. [[CrossRef](#)]
32. Maquiaveli, C.C.; Lucon-Júnior, J.F.; Brogi, S.; Campiani, G.; Gemma, S.; Vieira, P.C.; Silva, E.R. Verbascoside Inhibits Promastigote Growth and Arginase Activity of *Leishmania amazonensis*. *J. Nat. Prod.* **2016**, *79*, 1459–1463. [[CrossRef](#)]
33. da Silva, E.R.; da Silva, M.F.L.; Fischer, H.; Mortara, R.A.; Mayer, M.G.; Framesqui, K.; Silber, A.M.; Floeter-Winter, L.M. Biochemical and biophysical properties of a highly active recombinant arginase from *Leishmania (Leishmania) amazonensis* and subcellular localization of native enzyme. *Mol. Biochem. Parasitol.* **2008**, *159*, 104–111. [[CrossRef](#)]
34. Fawcett, J.K.; Scott, J.E. A Rapid and Precise Method for the Determination of Urea. *J. Clin. Pathol.* **1960**, *13*, 156–159. [[CrossRef](#)] [[PubMed](#)]
35. Mervin, L.H.; Afzal, A.M.; Drakakis, G.; Lewis, R.; Engkvist, O.; Bender, A. Target prediction utilising negative bioactivity data covering large chemical space. *J. Cheminform.* **2015**, *7*, 51. [[CrossRef](#)] [[PubMed](#)]
36. Mervin, L.H.; Bulusu, K.C.; Kalash, L.; Afzal, A.M.; Svensson, F.; Firth, M.A.; Barrett, I.; Engkvist, O.; Bender, A. Orthologue chemical space and its influence on target prediction. *Bioinformatics* **2018**, *34*, 72–79. [[CrossRef](#)]
37. Altschul, S.F.; Gish, W.; Miller, W.; Myers, E.W.; Lipman, D.J. Basic local alignment search tool. *J. Mol. Biol.* **1990**, *215*, 403–410. [[CrossRef](#)]
38. Simossis, V.A.; Heringa, J. PRALINE: A multiple sequence alignment toolbox that integrates homology-extended and secondary structure information. *Nucleic Acids Res.* **2005**, *33*, W289–W294. [[CrossRef](#)]
39. Varadi, M.; Anyango, S.; Deshpande, M.; Nair, S.; Natassia, C.; Yordanova, G.; Yuan, D.; Stroe, O.; Wood, G.; Laydon, A.; et al. AlphaFold Protein Structure Database: Massively expanding the structural coverage of protein-sequence space with high-accuracy models. *Nucleic Acids Res.* **2022**, *50*, D439–D444. [[CrossRef](#)]
40. Jumper, J.; Evans, R.; Pritzel, A.; Green, T.; Figurnov, M.; Ronneberger, O.; Tunyasuvunakool, K.; Bates, R.; Žídek, A.; Potapenko, A.; et al. Highly accurate protein structure prediction with AlphaFold. *Nature* **2021**, *596*, 583–589. [[CrossRef](#)]
41. Jones, G.; Willett, P.; Glen, R.C.; Leach, A.R.; Taylor, R. Development and validation of a genetic algorithm for flexible docking. *J. Mol. Biol.* **1997**, *267*, 727–748. [[CrossRef](#)] [[PubMed](#)]
42. Laskowski, R.A.; MacArthur, M.W.; Moss, D.S.; Thornton, J.M. PROCHECK: A program to check the stereochemical quality of protein structures. *J. Appl. Crystallogr.* **1993**, *26*, 283–291. [[CrossRef](#)]
43. Wiederstein, M.; Sippl, M.J. ProSA-web: Interactive web service for the recognition of errors in three-dimensional structures of proteins. *Nucleic Acids Res.* **2007**, *35*, W407–W410. [[CrossRef](#)] [[PubMed](#)]
44. Sippl, M.J. Recognition of errors in three-dimensional structures of proteins. *Proteins Struct. Funct. Bioinform.* **1993**, *17*, 355–362. [[CrossRef](#)] [[PubMed](#)]
45. Hanwell, M.D.; Curtis, D.E.; Lonie, D.C.; Vandermeersch, T.; Zurek, E.; Hutchison, G.R. Avogadro: An advanced semantic chemical editor, visualization, and analysis platform. *J. Cheminform.* **2012**, *4*, 17. [[CrossRef](#)] [[PubMed](#)]
46. Schrodinger, L. The PyMOL Molecular Graphics System. Available online: <https://pymol.org/> (accessed on 20 April 2022).
47. Dassault Systèmes BIOVIA, Discovery Studio Modeling Environment. Available online: <https://www.3ds.com/products-services/biovia/products/molecular-modeling-simulation/biovia-discovery-studio/> (accessed on 20 April 2022).

**Disclaimer/Publisher’s Note:** The statements, opinions and data contained in all publications are solely those of the individual author(s) and contributor(s) and not of MDPI and/or the editor(s). MDPI and/or the editor(s) disclaim responsibility for any injury to people or property resulting from any ideas, methods, instructions or products referred to in the content.